
Universal Adversarial Audio Perturbations

Sajjad Abdoli

Luiz G. Hafemann

Jérôme Rony

Ismail Ben Ayed

Patrick Cardinal

Alessandro L. Koerich

École de Technologie Supérieure
Université du Québec
H3C 1K, Montreal, QC, Canada

sajjad.abdoli.1@ens.etsmtl.ca, luiz.gh@mailbox.org, jerome.rony@gmail.com
ismail.benayed@etsmtl.ca, patrick.cardinal@etsmtl.ca, alessandro.koerich@etsmtl.ca

Abstract

We demonstrate the existence of universal adversarial perturbations, which can fool a family of audio processing architectures, for both targeted and untargeted attacks. To the best of our knowledge, this is the first study on generating universal adversarial perturbations for audio processing systems. We propose two methods for finding such perturbations. The first method is based on an iterative, greedy approach that is well-known in computer vision: it aggregates small perturbations to the input so as to push it to the decision boundary. The second method, which is the main technical contribution of this work, is a novel penalty formulation, which finds targeted and untargeted universal adversarial perturbations. Differently from the greedy approach, the penalty method minimizes an appropriate objective function on a batch of samples. Therefore, it produces more successful attacks when the number of training samples is limited. Moreover, we provide a proof that the proposed penalty method theoretically converges to a solution that corresponds to universal adversarial perturbations. We report comprehensive experiments, showing attack success rates higher than 91.1% and 74.7% for targeted and untargeted attacks, respectively.

1 Introduction

Deep learning models achieve state-of-the-art performance in various problems, notably in image recognition [1], natural language processing [2, 3] and speech processing [4, 5]. However, recent studies have demonstrated that such systems are vulnerable to adversarial attacks [6–9]. Adversarial examples are carefully perturbed input samples that can fool the detection system at test time [10, 6], posing security and reliability concerns for such systems. The threat of such attacks have been mainly addressed for computer vision tasks [9].

End-to-end audio processing systems have been gaining more attention recently [11–14]. In such systems, the input to the classifier is the audio signal. Moreover, there have been some studies that embed traditional signal processing techniques into the layers of Convolutional Neural Network (CNN) [15–17]. For such audio processing systems, the effect of adversarial attacks is not widely addressed [18]. Creating attacks on audio processing systems is challenging, due mainly to the signal variability in the time domain [18].

Moosavi-Dezfooli *et al.* [19] have shown the existence of *universal* adversarial perturbation, which, when added to an input image, causes the input to be misclassified with high probability. For these

universal attacks, the generated vector is independent from the input samples. However, to our knowledge, the existence of such vectors for audio classifiers has not been studied yet [18].

In this paper, we demonstrate the existence of universal adversarial perturbations, which can fool a family of audio processing architectures, for both targeted and untargeted attacks. To the best of our knowledge, this is the first study on generating universal adversarial perturbations for audio processing systems. We propose two methods for finding such perturbations. The first method is based on the greedy-approach principle of [19]: it finds the minimum perturbation that sends the samples to the decision boundary. The second method, which is the main technical contribution of this work, is a novel penalty formulation, which finds targeted and untargeted universal adversarial perturbations. Differently from the greedy approach, the penalty method minimizes an appropriate objective function on a batch of samples. Therefore, it produces more successful attacks when the number of training samples are limited. Moreover, we provide a proof that the proposed penalty method theoretically converges to a solution that corresponds to universal adversarial perturbations. Both methods are evaluated on a family of audio classifiers based on deep models for environmental sound classification. The experimental results have shown that both methods can attack the target models with a high success rate.

This paper is organized as follows: Section 2 presents an overview of adversarial attacks on deep learning models. Section 3 presents the proposed methods to craft universal audio adversarial perturbations. Section 4 presents the dataset and the target models used to evaluate the proposed methods, while the experimental results are presented in Section 5. The conclusion and perspective of future work is presented in the last section.

2 Adversarial Machine Learning

Research on adversarial attacks has attracted considerable attention recently, due to its impact on the reliability of a breadth of deep learning models. These attacks were mostly investigated in computer vision [8]. For a given image \mathbf{x} , an attack can find a small perturbation δ , often imperceptible to a human observer, so that a sample $\tilde{\mathbf{x}} = \mathbf{x} + \delta$ is misclassified by a deep network [6, 20, 21]. The attacker’s goal may cover a wide range of threats like *privacy* violation, *availability* violation and *integrity* violation [10]. Moreover, the attacker’s goal may be *specific* (targeted), with samples misclassified as a specific class or *generic* (untargeted), where the attacker simply wants to have a sample classified differently from the true class [10]. Attacks generated by targeting one classifier are often *transferable* to other classifiers (i.e. induce misclassification on them) [22], even if they have different architectures and do not use the same training set [6]. It was later shown that such attacks can also be applied in the physical world. For instance, Kurakin *et al.* [23] showed that printed adversarial examples were still misclassified after being captured by a camera; Athalye *et al.* [24] presented a method to generate adversarial examples that are robust under translation and scale transformations, showing that such attacks induce misclassification even when the samples correspond to different viewpoints.

Research on adversarial attacks on audio classification systems is quite recent. Some studies focused mainly on providing inaudible and hidden targeted attacks on the systems. In such attacks, new audio samples are synthesized, instead of adding perturbations to actual input samples [25, 26]. Other works focus on untargeted attacks on speech and music processing systems [27, 28]. Du *et al.* [29] proposed a method based on Particle Swarm Optimization (PSO) for targeted and untargeted attacks. They evaluated their attacks on a range of applications like speech command recognition, speaker recognition, sound event detection and music genre classification. Alzantot *et al.* [30] proposed a similar approach that uses a genetic algorithm for crafting targeted black-box attacks on a speech command classification system [31], which achieved 87% of success. Carlini *et al.* [18] proposed a targeted attack on the speech processing system DeepSpeech [11], which is a state-of-the-art speech-to-text transcription neural network. A penalty method is used in such attacks, which achieved 100% of success. Most studies consider that the attacker can directly manipulate the input samples of the classifiers. Crafting audio attacks that can work on the physical world (i.e. played over-the-air) presents challenges such as being robust to background noise and reverberations. Yakura *et al.* [32] showed that over-the-air attacks are possible, at least for a dataset of short phrases. Qin *et al.* [33] also reported successful adversarial attacks on automatic speech recognition system, which remain effective after applying realistic simulated environmental distortions.

Universal adversarial perturbations are effective type of attacks [19] because they can be generated once since the additive noise is independent of the input samples, and it can cause any sample to be misclassified by a deep model. Moosavi-Dezfooli *et al.* [19] proposed a greedy algorithm to provide such perturbations for untargeted attacks. The perturbation is generated by aggregating atomic perturbation vectors, which send the data points to the decision boundary of the classifier. Recently, Moosavi-Dezfooli *et al.* [34] provided a formal relationship between the geometry of the decision boundary and robustness to universal perturbations. They have also shown theoretically the strong vulnerability of state-of-the-art deep models to universal perturbations. Metzen *et al.* [35] generalized this idea to provide attacks against semantic image segmentation models. Recently, Behjati *et al.* [36] generalized this idea to attack a text classifier in both targeted and non-targeted scenarios. In a different approach, Hayes *et al.* [37] proposed a generative model for providing such universal perturbations. For audio processing systems, the impact of such perturbations can be very strong if these perturbations can be played over the air even without knowing what the test samples would look like. Although some robust adversarial audio attacks have been proposed, most of them are untargeted attacks that aim at fooling a classifier. Besides, most of the attacks consider specific target architectures.

3 Universal Audio Adversarial Perturbations

In this section, we formalize the problem of crafting universal audio adversarial perturbations, and propose two methods for finding such perturbations. The first method is based on the greedy-approach principle of [19]: it finds the minimum perturbation that sends the samples to the decision boundary of the classifier or inside the boundary of the target class for untargeted and targeted perturbations. The second method, which is the main technical contribution of this work, is a penalty formulation, which finds a universal perturbation vector that minimizes an objective function.

Let μ be the distribution of audio samples in \mathbb{R}^d and $\hat{k}(\mathbf{x}) = \arg \max_y \mathbb{P}(y|\mathbf{x}, \theta)$ be a classifier that predicts the correct class of the audio sample \mathbf{x} , where y is the true label of \mathbf{x} and θ denotes the parameters of the classifier. Our goal is to find a vector \mathbf{v} that once added to the audio samples can fool the classifier for most of the samples. This perturbation vector is called universal as it is a fixed noise that is independent of the audio samples and therefore it can be added to any sample in order to fool a classifier. The problem can be defined such that $\hat{k}(\mathbf{x} + \mathbf{v}) \neq \hat{k}(\mathbf{x})$ and for a targeted attack, $\hat{k}(\mathbf{x} + \mathbf{v}) = y_t$, where y_t denotes the target class. In this context, the universal perturbation is a vector with a sufficiently small l_p norm, where $p \in [1, \infty)$, which satisfies two constraints [19]: $\|\mathbf{v}\|_p \leq \xi$ and $\mathbb{P}_{\mathbf{x} \sim \mu}(\hat{k}(\mathbf{x} + \mathbf{v}) \neq \hat{k}(\mathbf{x})) \geq 1 - \delta$, where ξ controls the magnitude of the perturbation and δ controls the desired fooling rate. For a targeted attack, the second constraint is defined as $\mathbb{P}_{\mathbf{x} \sim \mu}(\hat{k}(\mathbf{x} + \mathbf{v}) = y_t) \geq 1 - \delta$.

3.1 Iterative Greedy Algorithm

Let $X = \{\mathbf{x}_1, \dots, \mathbf{x}_m\}$ be a set of m audio files sampled from the distribution μ . The greedy algorithm proposed by Moosavi-Dezfooli *et al.* [19] gradually crafts adversarial perturbations in an iterative manner. For untargeted attacks, at each iteration the algorithm finds the minimal perturbation $\Delta \mathbf{v}_i$ that pushes the sample \mathbf{x}_i to the decision boundary and adds the current perturbation to the universal perturbation. In this study, a targeted version of the algorithm is also proposed such that the universal perturbation added to the sample must push it inside the decision boundary of the target class. In more details, if the universal perturbation does not fool the sample, an extra $\Delta \mathbf{v}_i$ is found and aggregated to the universal perturbation by solving the following minimization problems for untargeted and targeted respectively:

$$\Delta \mathbf{v}_i \leftarrow \arg \min_{\mathbf{r}} \|\mathbf{r}\|_2 \text{ s.t. } \hat{k}(\mathbf{x}_i + \mathbf{v} + \mathbf{r}) \neq \hat{k}(\mathbf{x}_i), \quad (1)$$

$$\Delta \mathbf{v}_i \leftarrow \arg \min_{\mathbf{r}} \|\mathbf{r}\|_2 \text{ s.t. } \hat{k}(\mathbf{x}_i + \mathbf{v} + \mathbf{r}) = y_t, \quad (2)$$

In order to find $\Delta \mathbf{v}_i$ for each sample of the dataset, any attack that misclassifies the sample such as Carlini and Wanger L2 attack [8] or Decoupled Direction and Norm (DDN) attack [38] can be used. Moosavi-Dezfooli *et al.* [39] used Deepfool for finding such a vector.

In order to satisfy the first constraint ($\|\mathbf{v}\|_p \leq \xi$), the universal perturbation is projected on l_p ball of radius ξ and centered at 0. The projection is formulated as:

$$\mathcal{P}_{p,\xi}(\mathbf{v}) = \arg \min_{\mathbf{v}'} \|\mathbf{v} - \mathbf{v}'\|_2 \text{ s.t. } \|\mathbf{v}'\|_p \leq \xi \quad (3)$$

The termination criteria for the algorithm is defined such that the fooling rate on the perturbed training set exceeds a threshold $1 - \delta$. In this protocol, the algorithm stops for untargeted perturbations when:

$$\text{Err}(X, \mathbf{v}) := \frac{1}{m} \sum_{i=1}^m \mathbb{1}_{\hat{k}(\mathbf{x}_i + \mathbf{v}) \neq \hat{k}(\mathbf{x}_i)} \geq 1 - \delta \quad (4)$$

For a targeted attack, we replace the inequality $\hat{k}(\mathbf{x}_i + \mathbf{v}) \neq \hat{k}(\mathbf{x}_i)$ by $\hat{k}(\mathbf{x}_i + \mathbf{v}) = y_t$ in Equation 4.

3.2 Proposed Penalty Method

In this section a penalty method is proposed to find the solution of crafting universal adversarial perturbations. The method minimizes an appropriate objective function on a batch of samples from a dataset. In case of noise perception in audio systems, the level of noise perception can be measured using a realistic metric such as decibel (dB) [18]. Therefore, dB is used instead of L_p norm. In this study, such a measure is used as one of the targets of the optimization problem and one of the goals is to minimize the pressure level of the perturbation which is measured in dB. The problem of crafting a universal perturbation in a targeted attack can be reformulated as the following constrained optimization problem:

$$\begin{aligned} & \min dB(\mathbf{v}) \\ \text{s.t. } & y_t = \arg \max_y \mathbb{P}(y|\mathbf{x}_i + \mathbf{v}, \theta) \text{ and } 0 \leq \mathbf{x}_i + \mathbf{v} \leq 1 \quad \forall i \end{aligned} \quad (5)$$

where θ denotes the hyperparameters of the classifier. For untargeted attacks, we use $y_i \neq \arg \max_y \mathbb{P}(y|\mathbf{x}_i + \mathbf{v}, \theta)$, where y_i is the true label of the sample. The constraint on \mathbf{v} is proposed to ensure that the modification on the original signal produces a valid range. This box constraint should be valid for all audio samples: $0 \leq \mathbf{x}_i + \mathbf{v} \leq 1$. The power of noise in dB is computed as follows:

$$dB(\mathbf{v}) = 20 \log P(\mathbf{v}), \quad (6)$$

where $P(\mathbf{v})$ is the power of the signal of length N , which is given by:

$$P(\mathbf{v}) = \sqrt{\frac{1}{N} \sum_{n=1}^N v_n^2}, \quad (7)$$

where v_n denotes the n_{th} component of vector \mathbf{v} . We introduce a new parameter \mathbf{w} to ensure that the box constraint of the problem is held:

$$\mathbf{w}_i = \frac{1}{2}(\tanh(\mathbf{x}_i + \mathbf{v}) + 1), \quad (8)$$

Since $-1 \leq \tanh(\mathbf{x}_i + \mathbf{v}) \leq 1$ then $0 \leq \mathbf{w}_i \leq 1$ and the solution will be valid according to the box constraint. To solve this optimization problem, we propose a penalty method that optimizes the following objective function:

$$L(\mathbf{w}_i, \mathbf{v}; t) = \min \{dB(\mathbf{v}) + c.G(\mathbf{w}_i)\}, G(\mathbf{w}_i) = \max(\max_{j \neq t} \{f(\mathbf{w}_i)_j\} - f(\mathbf{w}_i)_t, -\kappa) \quad (9)$$

where t is the target class, $f(\mathbf{w}_i)_j$ is the output of the pre-softmax layer (logit) of the neural network for class j , and κ is a confidence value that controls the confidence level of sample misclassification.

This formulation enables the attacker to control the confidence level of the attack. For untargeted attacks, we modify the objective function in Eq. (9) as follows:

$$L(\mathbf{w}_i, \mathbf{v}; y_i) = \min \{dB(\mathbf{v}) + c.G(\mathbf{w}_i)\}, G(\mathbf{w}_i) = \max(f(\mathbf{w}_i)_{y_i} - \max_{j \neq y_i} \{f(\mathbf{w}_i)_j\}, -\kappa) \quad (10)$$

where y_i is the true label for the i_{th} sample of the batch. At iteration k , the algorithm solves the unconstrained minimization problem, $\mathbf{v}_k = \arg \min_{\mathbf{v}} \{dB(\mathbf{v}) + c.G(\mathbf{w}_i)\}$. Function $G(\mathbf{w}_i)$ is a penalty function which for targeted attack with $\kappa = 0$, must satisfy:

$$\begin{aligned} G(\mathbf{w}_i) &= 0 & \text{if } y_t = \arg \max_y \mathbb{P}(y|\mathbf{x}_i + \mathbf{v}, \theta), \\ G(\mathbf{w}_i) &> 0 & \text{if } y_t \neq \arg \max_y \mathbb{P}(y|\mathbf{x}_i + \mathbf{v}, \theta), \end{aligned} \quad (11)$$

The same properties of the penalty function are also valid for untargeted perturbations.

The Adam optimization algorithm [40] is used to minimize this objective function. Several other optimization algorithms like AdaGrad [41], standard gradient descent, gradient descent with Nesterov momentum [42] and RMSProp [43] were also evaluated. They produce relatively similar solutions but Adam was selected since it converges in fewer iterations.

Signal to Noise Ratio (SNR) is used as a metric to measure the level of the noise with respect to the original signal. This metric is used for measuring the level of the perturbation on the signal after adding the universal perturbation. This measure is also used in previous works for evaluating the quality of the generated adversarial audio attacks [28, 29]. This measure is defined as:

$$SNR_{dB}(\mathbf{x}, \mathbf{v}) = 20 \cdot \log_{10} \frac{P(\mathbf{x})}{P(\mathbf{v})} \quad (12)$$

where $P(\cdot)$ is the power of the signal defined in Eq. (7). Higher SNRs indicate that lower level of noise is added to the audio sample by the universal adversarial perturbation.

Algorithm 1 presents the pseudo-code of the proposed penalty method. The algorithm minimizes the objective function introduced in Eq. (9) or Eq. 10 using a set of training samples and the Adam optimizer [40, 43].

Theorem 1: Let $\{\mathbf{v}^k\}$, $k = 1, \dots, \infty$ be the sequence generated by the proposed penalty method in Algorithm 1. Let $\bar{\mathbf{v}}$ be the limit point of $\{\mathbf{v}^k\}$. Then any limit point of the sequence is a solution to the original optimization problem defined in Eq. (5).

Proof: Refer to supplementary material.

4 Experimental Protocol

The UrbanSound8k dataset [44] is used for training the target models and crafting the adversarial attacks. This dataset consists of 7.3 hours of audio recordings split into 8,732 audio clips of up to four seconds. For this study, we have used about three-second audio segments downsampled to 16 kHz for training and evaluating the models as well as for generating adversarial perturbations. Therefore, each audio sample is represented by a 50,999-dimensional array. The dataset was split into training (80%), validation (10%) and test (10%). For generating perturbations, 1,000 samples of the training set were randomly selected and the perturbations were evaluated on the whole test set (874 samples).

We have chosen a family of diverse end-to-end architectures as our target models. This selection is based on choosing architectures which might learn representations directly from the audio signal. We briefly describe the architecture of each model as follows. A detailed description of the architectures can be found in supplementary material.

1D CNN Rand [45]: This model consists of five one-dimensional convolutional layers (CL). The output of CLs is used as input to two fully connected (FC) layers followed by an output layer with softmax activation function. The weights of all of the layers are initialized randomly. This model is proposed by Abdoli *et al.* [45] for environmental sound classification.

Algorithm 1: Penalty method for universal adversarial audio perturbations.

Input: Data points $X = \{\mathbf{x}_1, \dots, \mathbf{x}_m\}$ with corresponding original labels Y , desired fooling rate on perturbed samples δ , Target class t (for targeted attacks)

Output: Universal perturbation signal \mathbf{v}

```
1 initialize  $\mathbf{v} \leftarrow 0$ ,
2 while  $\text{Err}(X, \mathbf{v}) \leq 1 - \delta$  do
3   Sample a mini-batch of size  $S$  from  $(X, Y)$ 
4    $\mathbf{g} \leftarrow 0$ 
5   for  $i \leftarrow 1$  to  $S$  do
6     Compute the transformation of the perturbed signal for each sample  $i$  from mini-batch:
        $\mathbf{w}_i = \frac{1}{2}(\tanh(\mathbf{x}_i + \mathbf{v}) + 1)$ ,
       Compute the gradient of the objective function, i.e., Eq. (9) or Eq. (10), w.r.t.  $\mathbf{w}_i$ :
7     if targeted attack: then
8        $\mathbf{g} \leftarrow \mathbf{g} + \frac{\partial L(\mathbf{w}_i, \mathbf{v}; t)}{\partial \mathbf{w}_i}$ 
9     else
10       $\mathbf{g} \leftarrow \mathbf{g} + \frac{\partial L(\mathbf{w}_i, \mathbf{v}; y_i)}{\partial \mathbf{w}_i}$ 
11  Compute update  $\Delta \mathbf{v}$  using  $\mathbf{g}$  according to the Adam update rule [40]
    apply update:  $\mathbf{v} \leftarrow \mathbf{v} + \Delta \mathbf{v}$ 
return  $\mathbf{v}$ 
```

1D CNN Gamma [45]: This model is similar to 1D CNN Rand except that it employs a Gammatone filter-bank at the first layer of the model. Furthermore, this layer is kept frozen during the training process. Gammatone filters are used to decompose the input signal to appropriate frequency bands. This model is also proposed by Abdoli *et al.* [45] for environmental sound classification.

ENVnet-V2: Tokozume *et al.* [46] proposed an architecture for sound recognition. The model was slightly modified to make it compatible with the input size of the samples of UrbanSound8k dataset. This architecture uses raw audio signal as input. This model extracts short-time frequency features by using two one-dimensional CLs followed by a pooling layer (PL). It then swaps axes and convolves the features in time and frequency domain using five two-dimensional CLs. After, two FC layers and an output layer with softmax activation function complete the network.

SincNet: Ravanelli *et al.* [15] proposed an end-to-end architecture for sound processing which extracts from the audio signal meaningful features at the first layer. In this model, several sinc functions are used as band-pass filters and only low and high cutoff frequencies are learned from audio. After that, two one-dimensional CLs are applied. Two FC layers followed by a output layer with softmax activation are used for classification.

SincNet+VGG19: This model uses sinc filters to extract features from the raw audio signal as in SincNet [15]. After applying one-dimensional maxpooling layer the output is stacked along time axis to form a 2D representation. This time-frequency representation is used as the input to a VGG19 [47] network followed by a FC layer and an output layer with softmax activation for classification. This time-frequency representation resembles spectrogram representation of the audio signal.

For the iterative method, several parameters must be chosen. In order to find the minimal perturbation $\Delta \mathbf{v}_i$, we used the DDN L_2 attack [38]. This attack is designed to efficiently find small perturbations that fool the model. The difference with DeepFool [39] is that it can be used for both untargeted and targeted attacks, extending the iterative method to the targeted scenario. DDN was used with a budget of 50 steps and an initial norm of 0.2. Results are reported for $p = \infty$ and we set $\xi = 0.09$. This value is set to craft perturbations in which the norm is much lower than the norm of the audio samples in the dataset ¹.

For evaluating the penalty method, we set the penalty term $c = 0.002$ and the confidence value $\kappa = 5$ for all models. Figure 1 shows the effect of different confidence values on both mean Attack Success Rate (ASR) and mean SNR for targeted and untargeted attacks on the ENVnet-V2 model [46] for the test set. As shown in Equation 4, ASR is defined by dividing the number of the misclassified samples

¹the l_∞ norm of the samples of the dataset is 0.88.

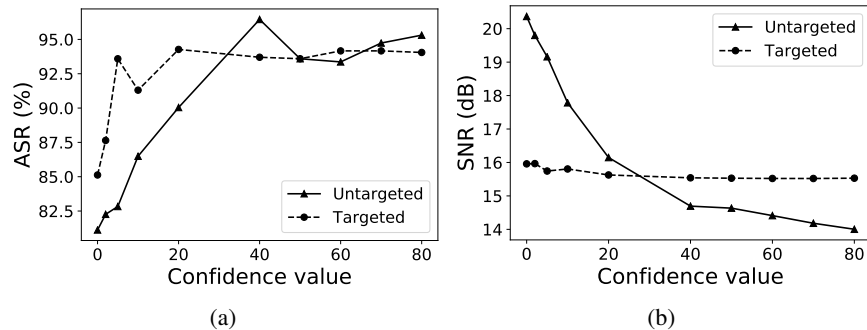


Figure 1: Effect of different confidence values on (a) mean ASR and (b) mean SNR for targeted and untargeted attacks. ENVnet-V2 [46] is used as target model.

by the total number of samples. For this experiment, only 500 training samples are used. For targeted attacks, the target class is "Gun shot". Figure 1 shows that the confidence value increases as the ASR increases. However, the SNR also decreases in the same way. For both iterative and penalty methods, we set the desired fooling rate on perturbed training samples to $\delta = 0.1$. Both algorithms terminate execution whether they achieve the desired fooling ratio or they reach 100 iterations. Both algorithms have been trained and tested using a TITAN Xp GPU.

| Method | Model | Targeted Attack | | | Untargeted Attack | | |
|-----------|---------------|-----------------|--------------|----------|-------------------|--------------|----------|
| | | Training Set | | Test Set | Training Set | | Test Set |
| | | ASR | ASR | SNR (dB) | ASR | ASR | SNR (dB) |
| Iterative | 1D CNN Rand | 0.982 | 0.959 | 16.428 | 0.909 | 0.858 | 16.793 |
| | 1D CNN Gamma | 0.983 | 0.911 | 17.373 | 0.927 | 0.747 | 16.065 |
| | ENVnet-V2 | 0.984 | 0.961 | 17.983 | 0.924 | 0.773 | 15.415 |
| | SincNet | 1.000 | 0.999 | 19.317 | 0.915 | 0.933 | 16.979 |
| | SincNet+VGG19 | 0.990 | 0.973 | 19.083 | 0.911 | 0.845 | 19.616 |
| Penalty | 1D CNN Rand | 0.961 | 0.954 | 15.967 | 0.921 | 0.897 | 15.270 |
| | 1D CNN Gamma | 0.954 | 0.927 | 16.169 | 0.917 | 0.810 | 15.659 |
| | ENVnet-V2 | 0.971 | 0.952 | 16.990 | 0.912 | 0.875 | 18.029 |
| | SincNet | 0.998 | 1.000 | 17.988 | 0.911 | 0.947 | 15.910 |
| | SincNet+VGG19 | 0.945 | 0.940 | 17.709 | 0.918 | 0.881 | 17.393 |

Table 1: Mean ASR and mean SNR on train and test sets for untargeted and targeted perturbations.

5 Results

Table 1 shows the results of the iterative and penalty-based methods against the 5 models considered in this study. We evaluate both targeted and untargeted attacks in terms of mean ASR (Attack Success Ratio) on training and test set, as well as mean SNR (Signal to Noise ratio) of the perturbed samples of the test set. For targeted attacks, the iterative method produced a slightly better ASR for targeting 1D CNN Rand, ENVnet-V2 and SincNet+VGG19 models, while the penalty method produces slightly higher ASR for targeting 1D CNN Gamma and SincNet. Both methods produce relatively similar mean SNR on the test set.

For both methods, the crafted universal perturbations generalize well to the test set, and we observe a relatively low difference in ASR on the training and test sets. Table 1 also shows the results of untargeted universal adversarial perturbations on target models. The penalty method produces better mean ASR on test set for targeting all of the proposed target models. Similar to targeted attack scenario, there is no significant difference between the mean SNR of the perturbed audio signals produced by two models. Here, it is also observed that perturbation vectors produced on the training set is well transferable to the test set. The detailed results of the targeted attack scenario for each model is reported in the supplementary material.

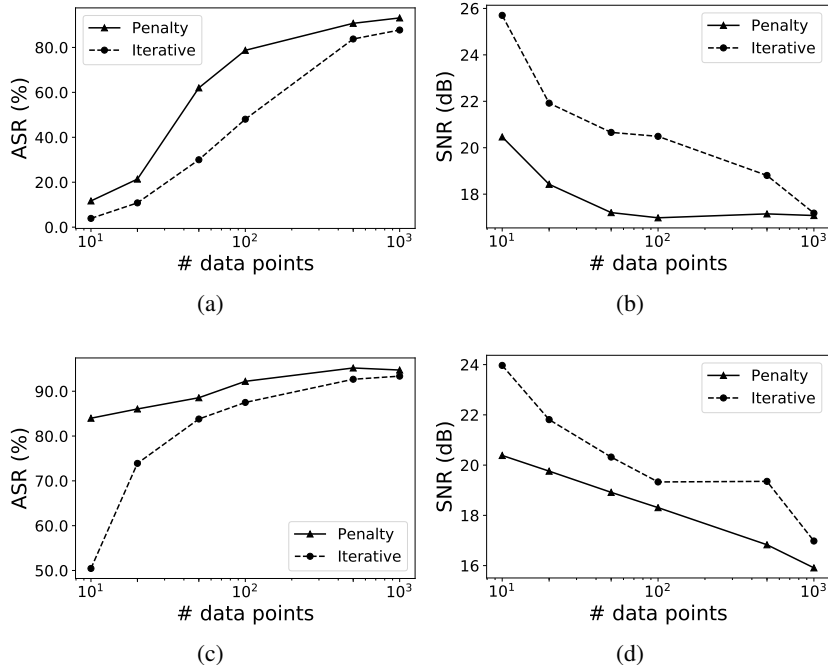


Figure 2: Targeted and untargeted attack success rate and mean SNR on the test set versus the number of training data points. Targeted attack: (a) ASR on 1D CNN Gamma model; (b) mean SNR on inputs of 1D CNN Gamma model. Untargeted attack: (c) ASR on SincNet; (d) mean SNR on inputs of SincNet.

We now consider the influence of the number of training data points on the quality of the universal perturbations. Figure 2 shows the ASR and mean SNR achieved on the test set with different number of data points, considering two target models. Untargeted attack is evaluated on SincNet and targeted attack is evaluated on 1D CNN Gamma model. For targeted attack, the target class is "Gun shot". For both targeted and untargeted scenarios, penalty method produces better ASR when the perturbations are crafted with a lower number of data points. Iterative model produces perturbations with a slightly better mean SNR. However, this difference is perceptually negligible. For a better assessment of the perturbations produced by both proposed methods, several randomly chosen examples of perturbed audio samples are presented in supplementary material.

6 Conclusion and Future Work

In this study, we proposed an iterative method and a penalty method for generating targeted and untargeted universal adversarial audio perturbations. Both methods were used for attacking a diverse family of end-to-end audio classifiers based on deep models and the experimental results have shown that both methods can easily fool all models with a high success rate. It is also mathematically proven that the proposed penalty method converges to an optimal solution.

Although the generated perturbations can target the models with high success rate. In listening tests, the additive noise to the audio signal is detectable. Developing effective universal adversarial audio examples by the use of principle of auditory masking [33] to reduce the level of noise introduced by the adversarial perturbation is our current goal.

Different from image-based universal adversarial perturbations [48], the universal audio perturbations crafted in this study do not perform well in the physical world (played over-the-air). Combining the methods proposed in this paper with recent studies on generating robust adversarial attacks on several transformations on the audio signal [32, 33] may be a promising way to craft robust physical attacks against audio systems.

Moreover, conducting an extensive study of the transferability of the universal perturbations over proposed models is also an important direction for future work. The transferability of perturbations may be examined for targeted and untargeted scenarios [49].

Finally, proposing a defensive mechanism against such universal perturbations is also an important problem. Using methods like adversarial training [50] against such attacks is also considered as one of our future research directions.

Supplementary Material

A Proof of Theorem 1

Theorem 1: Let $\{\mathbf{v}^k\}$, $k = 1, \dots, \infty$, be the sequence generated by the proposed penalty method. Let $\bar{\mathbf{v}}$ be the limit point of $\{\mathbf{v}^k\}$, then any limit point of the sequence is a solution to the original optimization problem:

$$\begin{aligned} \min dB(\mathbf{v}) \\ \text{s.t. } y_t = \arg \max_y \mathbb{P}(y|\mathbf{x}_i + \mathbf{v}, \theta) \\ \text{and} \\ 0 \leq \mathbf{x}_i + \mathbf{v} \leq 1 \quad \forall \mathbf{x}_i. \end{aligned} \quad (13)$$

Before proving the Theorem 1, a useful lemma is presented and proved.

Lemma 1: let \mathbf{v}^* be the optimal value of the original constrained problem defined in Eq. (5). Then $dB(\mathbf{v}^*) \geq L(\mathbf{w}_i^k, \mathbf{v}^k; t) \geq dB(\mathbf{v}^k) \forall k$.

Proof of Lemma 1:

$$\begin{aligned} dB(\mathbf{v}^*) &= dB(\mathbf{v}^*) + c.G(\mathbf{w}_i^*) && (\because G(\mathbf{w}_i^*) = 0) \\ &\geq dB(\mathbf{v}^k) + c.G(\mathbf{w}_i^k) && (\because c > 0, G(\mathbf{w}_i^k) \geq 0, \mathbf{w}_i^k \text{ minimizes } L(\mathbf{w}_i^k, \mathbf{v}^k; t)) \\ &\geq dB(\mathbf{v}^k) \\ \therefore dB(\mathbf{v}^*) &\geq L(\mathbf{w}_i^k, \mathbf{v}^k; t) \geq dB(\mathbf{v}^k) \forall k \end{aligned}$$

Proof of Theorem 1. dB is a monotonically increasing function and continuous. Also, G is a hinge function, which is continuous. L is the summation of two continuous functions. Therefore, it is also a continuous function. The limit point of $\{\mathbf{v}^k\}$ is defined as: $\bar{\mathbf{v}} = \lim_{k \rightarrow \infty} \mathbf{v}^k$ and since function dB is a continuous function, $dB(\bar{\mathbf{v}}) = \lim_{k \rightarrow \infty} dB(\mathbf{v}^k)$. We can conclude that:

$$\begin{aligned} L^* &= \lim_{k \rightarrow \infty} L(\mathbf{w}_i^k, \mathbf{v}^k; t) \leq dB(\mathbf{v}^*) \quad (\because \text{Lemma 1}) \\ \Rightarrow L^* &= \lim_{k \rightarrow \infty} dB(\mathbf{v}^k) + \lim_{k \rightarrow \infty} c.G(\mathbf{w}_i^k) \leq dB(\mathbf{v}^*) \\ \Rightarrow L^* &= dB(\bar{\mathbf{v}}) + \lim_{k \rightarrow \infty} c.G(\mathbf{w}_i^k) \leq dB(\mathbf{v}^*) \end{aligned}$$

If \mathbf{v}^k is a feasible point for the constrained optimization problem defined in Eq. (5), then, from the definition of function $G(\cdot)$, one can conclude that $\lim_{k \rightarrow \infty} c.G(\mathbf{w}_i^k) = 0$. Then:

$$L^* = dB(\bar{\mathbf{v}}) \leq dB(\mathbf{v}^*)$$

$\therefore \bar{\mathbf{v}}$ is a solution of the problem defined in Eq. (5)

B Target models

In this study five types of models are targeted. For training all of the models categorical crossentropy is used as loss function and Adadelata [51] is used for optimizing the parameters of the models. In this section the complete description of the models is presented.

B.1 1D CNN Rand

Table 2 shows the configuration of 1D CNN Rand [45]. This model consists of 5 one dimensional convolutional layers. The number of the kernels of each convolutional layer is 16, 32, 64, 128 and 256. The size of the feature maps of each convolutional layer is 64, 32, 16, eight and four. The first, second and fifth convolutional layers are followed by a one dimensional max-pooling layer of size of eight, eight and four, respectively. The output of the second pooling layer is used as input to two Fully Connected (FC) layers on which a drop-out with probability of 0.5 is applied for both layers [52]. Relu is used as the activation function for all of the layers. The number of the neurons of the FC layers are 128 and 64. In order to reduce the over-fitting, batch normalization is applied after the activation function of each convolution layer [53]. The output of last fully connected layer is used as the input to a softmax layer with ten neurons for classification.

| Layer | Ksize | Stride | # of filters | Data shape |
|--------------|-------|--------|--------------|--------------|
| InputLayer | - | - | - | (50,999, 1) |
| Conv1D | 64 | 2 | 16 | (25,468, 16) |
| MaxPooling1D | 8 | 8 | 16 | (3,183, 16) |
| Conv1D | 32 | 2 | 32 | (1,576, 32) |
| MaxPooling1D | 8 | 8 | 32 | (197, 32) |
| Conv1D | 16 | 2 | 64 | (91, 64) |
| Conv1D | 8 | 2 | 128 | (42, 128) |
| Conv1D | 4 | 2 | 256 | (20, 256) |
| MaxPooling1D | 4 | 4 | 128 | (5, 256) |
| FC | - | - | 128 | (128) |
| FC | - | - | 64 | (64) |
| FC | - | - | 10 | (10) |

Table 2: 1D CNN Rand architecture.

B.2 1D CNN Gamma

This model is similar to 1D CNN Rand except a gammatone filter-bank is used for initialization of the filters of the first layer of this model [45]. Table 3 shows the configuration of this model. The filters of gammatone filter-bank is not trained during the backpropagation process. Sixty four filters are used to decompose the input signal into appropriate frequency bands. This filter-bank covers the frequency range between 100Hz to 8 kHz. After this layer, batch normalization is also applied [53].

B.3 ENVnet-V2

Table 4 shows the architecture of ENVnet-V2 [46]. This model extracts short-time frequency features from audio file by using two one dimensional convolutional layers each with 32 and 64 filters followed

| Layer | Ksize | Stride | # of filters | Data shape |
|--------------|-------|--------|--------------|--------------|
| InputLayer | - | - | - | (50,999, 1) |
| Conv1D | 512 | 1 | 64 | (50,488, 64) |
| MaxPooling1D | 8 | 8 | 64 | (6,311, 64) |
| Conv1D | 32 | 2 | 32 | (3,140, 32) |
| MaxPooling1D | 8 | 8 | 32 | (392, 32) |
| Conv1D | 16 | 2 | 64 | (189, 64) |
| Conv1D | 8 | 2 | 128 | (91, 128) |
| Conv1D | 4 | 2 | 256 | (44, 256) |
| MaxPooling1D | 4 | 4 | 128 | (11, 256) |
| FC | - | - | 128 | (128) |
| FC | - | - | 64 | (64) |
| FC | - | - | 10 | (10) |

Table 3: 1D CNN Gamma architecture

| Layer | Ksize | Stride | # of filters | Data shape |
|--------------|-------|--------|--------------|---------------|
| InputLayer | - | - | - | (50,999, 1) |
| Conv1D | 64 | 2 | 32 | (25,468, 32) |
| Conv1D | 16 | 2 | 64 | (12,727, 64) |
| MaxPooling1D | 64 | 64 | 64 | (198, 64) |
| swapaxes | - | - | - | (64, 128, 1) |
| Conv2D | (8,8) | (1,1) | 32 | (57, 191, 32) |
| Conv2D | (8,8) | (1,1) | 32 | (50, 184, 32) |
| MaxPooling2D | (5,3) | (5,3) | 32 | (10, 61, 32) |
| Conv2D | (1,4) | (1,1) | 64 | (10, 58, 64) |
| Conv2D | (1,4) | (1,1) | 64 | (10, 55, 64) |
| MaxPooling2D | (1,2) | (1,2) | 64 | (10, 27, 64) |
| Conv2D | (1,2) | (1,1) | 128 | (10, 26, 128) |
| FC | - | - | 4,096 | (4,096) |
| FC | - | - | 4,096 | (4,096) |
| FC | - | - | 10 | (10) |

Table 4: ENVnet-V2 architecture

| Layer | Ksize | Stride | # of filters | Data shape |
|--------------|-------|--------|--------------|--------------|
| InputLayer | - | - | - | (50,999, 1) |
| SincConv1D | 251 | 1 | 80 | (50,749, 80) |
| MaxPooling1D | 3 | 1 | 80 | (16,916, 80) |
| Conv1D | 5 | 1 | 60 | (16,912, 60) |
| MaxPooling1D | 3 | 1 | 60 | (5,637, 60) |
| Conv1D | 5 | 1 | 60 | (5,633, 60) |
| FC | - | - | 128 | (128) |
| FC | - | - | 64 | (64) |
| FC | - | - | 10 | (10) |

Table 5: SincNet architecture

by a one dimensional max-pooling layer. The model then swaps axes and convolve the features in time and frequency domain by the use of two two-dimensional convolutional layers each with 32 filters. After convolutional layers, a two dimensional max-pooling layer is used. After that, two other two dimensional convolutional layers followed by a max-pooling layer are used. After that, another two dimensional convolutional layer with 128 filters is used. After using two FC layers with 4096 neurons, a softmax layer is applied for classification. Drop-out with probability of 0.5 is also applied on FC layers [52]. Relu is also used as the activation function for all of the layers.

B.4 SincNet

Table 5 shows the architecture of SincNet [15]. In this model, 80 sinc functions are used as band-pass filters for decomposing the audio signal into appropriate frequency bands. After that, two one-dimensional convolutional layers with 80 and 60 filters are applied. Layer normalization [54] is also used after each convolutional layer. After each convolutional layer, max-pooling is also used. Two FC layers followed by a softmax layer is used for classification. Drop-out with probability of 0.5 is also used on FC layers [52]. Batch normalization [53] is also used after FC layers. In this model, all hidden layers use leaky-ReLU [55] non-linearities.

B.5 SincNet+VGG19

Table 6 shows the specification of this architecture. This model uses 227 Sinc filters to extract features from the raw audio signal as it is introduced in SincNet [15]. After applying one-dimensional max-pooling layer of size of 218 with stride of one, and layer normalization [54], the output is stacked along time axis to form a 2D representation. This time-frequency representation is used as the input to a VGG19 [47] network followed by a FC layer and softmax layer for classification. The parameters

| Layer | Ksize | Stride | # of filters | Data shape |
|--------------|-------|--------|--------------|---------------|
| InputLayer | - | - | - | (50,999, 1) |
| SincConv1D | 251 | 1 | 227 | (50,749, 1) |
| MaxPooling1D | 218 | 1 | 227 | (232, 1) |
| Reshape | - | - | - | (232, 227, 1) |
| VGG19 [47] | - | - | - | (7, 7, 512) |
| FC | - | - | 10 | (10) |

Table 6: SincNet+VGG19 architecture

of the VGG19 is the same as described in [47] and they are not changed in this study. The output of VGG19 is used as the input of a softmax layer with ten neurons for classification.

C Audio examples

Several randomly chosen examples of perturbed audio samples of Urbansound8k dataset [44] are also presented. The audio samples are perturbed based on two presented methods in this study. Targeted and untargeted perturbations are considered. Table 7 shows a list of the samples. Methodology of crafting the samples, target models, and also detected class of the sample by each model as well as the true class of the samples are presented.

| Sample | Detected Class | True Class | Target Model | Method | Targeted/Untargeted |
|-------------------|------------------|---------------|--------------|-----------|---------------------|
| JA_0_org.wav | jackhammer | jackhammer | SINCNet | N/A | N/A |
| JA_0_pert_pen.wav | gun_shot | jackhammer | SINCNet | penalty | targeted |
| JA_0_pert_itr.wav | gun_shot | jackhammer | SINCNet | iterative | targeted |
| SI_0_org.wav | siren | siren | SINCNet | N/A | N/A |
| SI_0_pert_itr.wav | car_horn | siren | SINCNet | iterative | targeted |
| SI_0_pert_pen.wav | car_horn | siren | SINCNet | penalty | targeted |
| ST_0_org.wav | street_music | street_music | SINCNet | N/A | N/A |
| ST_0_pert_pen.wav | air_conditioner | street_music | SINCNet | penalty | targeted |
| ST_0_pert_itr.wav | air_conditioner | street_music | SINCNet | iterative | targeted |
| DR_0_org.wav | drilling | drilling | SINCNet | N/A | N/A |
| DR_0_pert_pen.wav | siren | drilling | SINCNet | penalty | targeted |
| DR_0_pert_itr.wav | siren | drilling | SINCNet | iterative | targeted |
| CA_0_org.wav | car_horn | car_horn | SINCNet+VGG | N/A | N/A |
| CA_0_pert_itr.wav | siren | car_horn | SINCNet+VGG | iterative | targeted |
| CA_0_pert_pen.wav | siren | car_horn | SINCNet+VGG | penalty | targeted |
| JA_1_org.wav | jackhammer | jackhammer | SINCNet+VGG | N/A | N/A |
| JA_1_pert_itr.wav | dog_bark | jackhammer | SINCNet+VGG | iterative | untargeted |
| JA_1_pert_pen.wav | children_playing | jackhammer | SINCNet+VGG | penalty | untargeted |
| EN_0_org.wav | engine_idling | engine_idling | SINCNet+VGG | N/A | N/A |
| EN_0_pert_itr.wav | drilling | engine_idling | SINCNet+VGG | iterative | untargeted |
| EN_0_pert_pen.wav | drilling | engine_idling | SINCNet+VGG | penalty | untargeted |
| CA_1_org.wav | car_horn | car_horn | SINCNet+VGG | N/A | N/A |
| CA_1_pert_pen.wav | drilling | car_horn | SINCNet+VGG | penalty | untargeted |
| CA_1_pert_itr.wav | drilling | car_horn | SINCNet+VGG | iterative | untargeted |
| SI_1_org.wav | siren | siren | SINCNet+VGG | N/A | N/A |
| SI_1_pert_itr.wav | street_music | siren | SINCNet+VGG | iterative | untargeted |
| SI_1_pert_pen.wav | children_playing | siren | SINCNet+VGG | penalty | untargeted |

Table 7: List of examples of perturbed audio samples, Methodology of crafting the samples, target models, and also detected class of the sample by each model and the true class of the samples. The audio files belong to UrbanSound8k dataset [44]. N/A: Not Applicable

D Detailed targeted attack results

Table 8 to table 12 show the detailed ASR on train set and test set on the target models in targeted attack scenario. For each specific target class of UrbanSound8k [44] ASRs are reported. Mean SNRs of the inputs to the models after adding universal perturbation are also reported. The target classes are: Air conditioner (AI), Car horn (CA), Children playing (CH), Dog bark (DO), Drilling (DR), Engine (EN) idling, Gun shot (GU), Jackhammer (JA), Siren (SI), Street music (ST).

| Method | Target Classes | | | | | | | | | | |
|-----------|-------------------|--------------|--------------|--------------|--------------|--------------|--------------|--------------|--------------|--------------|--------------|
| | AI | CA | CH | DO | DR | EN | GU | JA | SI | ST | |
| Iterative | ASR train set | 0.943 | 0.997 | 0.953 | 0.994 | 0.996 | 0.994 | 0.988 | 0.977 | 0.990 | 0.996 |
| | ASR test set | 0.911 | 0.970 | 0.905 | 0.977 | 0.978 | 0.981 | 0.969 | 0.954 | 0.965 | 0.982 |
| | SNR (dB) test set | 14.760 | 16.520 | 15.519 | 17.839 | 16.681 | 15.735 | 18.389 | 16.165 | 15.673 | 17.006 |
| Penalty | ASR train set | 0.951 | 0.970 | 0.935 | 0.969 | 0.968 | 0.959 | 0.985 | 0.965 | 0.937 | 0.976 |
| | ASR test set | 0.953 | 0.962 | 0.918 | 0.951 | 0.967 | 0.961 | 0.981 | 0.967 | 0.926 | 0.965 |
| | SNR (dB) test set | 15.254 | 15.676 | 16.584 | 16.330 | 16.273 | 15.290 | 16.061 | 15.887 | 16.456 | 15.864 |

Table 8: ASR and mean SNR for targeting each label of UrbanSound8k [44] dataset. The target model is 1D CNN Rand.

| Method | | Target Classes | | | | | | | | | |
|-----------|-------------------|----------------|--------------|--------------|--------------|--------------|--------------|--------------|--------------|--------------|--------------|
| | | AI | CA | CH | DO | DR | EN | GU | JA | SI | ST |
| Iterative | ASR train set | 0.943 | 0.997 | 0.953 | 0.994 | 0.996 | 0.994 | 0.988 | 0.977 | 0.990 | 0.996 |
| | ASR test set | 0.911 | 0.970 | 0.905 | 0.977 | 0.978 | 0.981 | 0.969 | 0.954 | 0.965 | 0.982 |
| | SNR (dB) test set | 14.760 | 16.520 | 15.519 | 17.839 | 16.681 | 15.735 | 18.389 | 16.165 | 15.673 | 17.006 |
| Penalty | ASR train set | 0.951 | 0.970 | 0.935 | 0.969 | 0.968 | 0.959 | 0.985 | 0.965 | 0.937 | 0.976 |
| | ASR test set | 0.953 | 0.962 | 0.918 | 0.951 | 0.967 | 0.961 | 0.981 | 0.967 | 0.926 | 0.965 |
| | SNR (dB) test set | 15.254 | 15.676 | 16.584 | 16.330 | 16.273 | 15.290 | 16.061 | 15.887 | 16.456 | 15.864 |

Table 9: ASR and mean SNR for targeting each label of UrbanSound8k [44] dataset. The target model is 1D CNN Gamma.

| Method | | Target Classes | | | | | | | | | |
|-----------|-------------------|----------------|--------------|--------------|--------------|--------------|--------------|--------------|--------------|--------------|--------------|
| | | AI | CA | CH | DO | DR | EN | GU | JA | SI | ST |
| Iterative | ASR train set | 0.992 | 0.977 | 0.980 | 0.993 | 0.975 | 0.993 | 0.979 | 0.979 | 0.991 | 0.982 |
| | ASR test set | 0.977 | 0.960 | 0.965 | 0.971 | 0.950 | 0.969 | 0.954 | 0.963 | 0.974 | 0.937 |
| | SNR (dB) test set | 18.373 | 17.374 | 17.791 | 18.450 | 17.492 | 17.989 | 18.321 | 17.953 | 17.896 | 18.192 |
| Penalty | ASR train set | 0.964 | 0.964 | 0.975 | 0.977 | 0.981 | 0.963 | 0.977 | 0.950 | 0.990 | 0.971 |
| | ASR test set | 0.938 | 0.935 | 0.960 | 0.960 | 0.962 | 0.947 | 0.963 | 0.910 | 0.983 | 0.962 |
| | SNR (dB) test set | 18.327 | 16.645 | 18.529 | 16.135 | 15.985 | 17.291 | 15.672 | 17.257 | 16.844 | 17.219 |

Table 10: ASR and mean SNR for targeting each label of UrbanSound8k [44] dataset. The target model is ENVnet-V2.

| Method | | Target Classes | | | | | | | | | |
|-----------|-------------------|----------------|--------------|--------------|--------------|--------------|--------------|--------------|--------------|--------------|--------------|
| | | AI | CA | CH | DO | DR | EN | GU | JA | SI | ST |
| Iterative | ASR train set | 1.000 | 1.000 | 1.000 | 1.000 | 1.000 | 1.000 | 1.000 | 1.000 | 1.000 | 1.000 |
| | ASR test set | 0.998 | 0.999 | 1.000 | 1.000 | 1.000 | 1.000 | 1.000 | 1.000 | 0.999 | 0.997 |
| | SNR (dB) test set | 19.559 | 17.826 | 19.687 | 19.460 | 20.144 | 19.701 | 18.283 | 19.511 | 18.884 | 20.125 |
| Penalty | ASR train set | 1.000 | 0.989 | 1.000 | 1.000 | 1.000 | 1.000 | 0.994 | 0.999 | 0.998 | 1.000 |
| | ASR test set | 1.000 | 0.998 | 1.000 | 1.000 | 1.000 | 1.000 | 0.998 | 1.000 | 1.000 | 1.000 |
| | SNR (dB) test set | 17.813 | 17.404 | 18.328 | 18.187 | 17.906 | 18.103 | 17.540 | 18.343 | 17.883 | 18.379 |

Table 11: ASR and mean SNR for targeting each label of UrbanSound8k [44] dataset. The target model is SincNet.

| Method | | Target Classes | | | | | | | | | |
|-----------|-------------------|----------------|--------------|--------------|--------------|--------------|--------------|--------------|--------------|--------------|--------------|
| | | AI | CA | CH | DO | DR | EN | GU | JA | SI | ST |
| Iterative | ASR train set | 0.991 | 0.998 | 0.998 | 0.998 | 0.997 | 0.952 | 0.982 | 1.000 | 0.996 | 0.994 |
| | ASR test set | 0.975 | 0.987 | 0.987 | 0.986 | 0.978 | 0.928 | 0.957 | 0.981 | 0.986 | 0.969 |
| | SNR (dB) test set | 18.354 | 19.296 | 19.297 | 19.217 | 20.755 | 17.498 | 18.048 | 19.683 | 19.096 | 19.592 |
| Penalty | ASR train set | 0.960 | 0.965 | 0.974 | 0.900 | 0.982 | 0.906 | 0.950 | 0.968 | 0.931 | 0.916 |
| | ASR test set | 0.959 | 0.961 | 0.958 | 0.896 | 0.989 | 0.903 | 0.939 | 0.961 | 0.931 | 0.913 |
| | SNR (dB) test set | 16.968 | 18.293 | 18.049 | 18.448 | 18.373 | 16.270 | 17.037 | 18.103 | 17.733 | 17.819 |

Table 12: ASR and mean SNR for targeting each label of UrbanSound8k [44] dataset. The target model is SincNet+VGG.

References

- [1] Zhong-Qiu Zhao, Peng Zheng, Shou-tao Xu, and Xindong Wu, “Object detection with deep learning: A review,” *IEEE transactions on neural networks and learning systems*, 2019.
- [2] Michelle Yuan, Benjamin Van Durme, and Jordan L Ying, “Multilingual anchoring: Interactive topic modeling and alignment across languages,” in *Advances in Neural Information Processing Systems*, 2018, pp. 8653–8663.
- [3] Zichao Yang, Zhiting Hu, Chris Dyer, Eric P Xing, and Taylor Berg-Kirkpatrick, “Unsupervised text style transfer using language models as discriminators,” in *Advances in Neural Information Processing Systems*, 2018, pp. 7287–7298.
- [4] Ye Jia, Yu Zhang, Ron Weiss, Quan Wang, Jonathan Shen, Fei Ren, Patrick Nguyen, Ruoming Pang, Ignacio Lopez Moreno, Yonghui Wu, et al., “Transfer learning from speaker verification to multispeaker text-to-speech synthesis,” in *Advances in Neural Information Processing Systems*, 2018, pp. 4480–4490.
- [5] Yu-An Chung, Wei-Hung Weng, Schrasing Tong, and James Glass, “Unsupervised cross-modal alignment of speech and text embedding spaces,” in *Advances in Neural Information Processing Systems*, 2018, pp. 7354–7364.
- [6] Christian Szegedy, Wojciech Zaremba, Ilya Sutskever, Joan Bruna, Dumitru Erhan, Ian Goodfellow, and Rob Fergus, “Intriguing properties of neural networks,” *arXiv preprint arXiv:1312.6199*, 2013.
- [7] Ian J. Goodfellow, Jonathon Shlens, and Christian Szegedy, “Explaining and Harnessing Adversarial Examples,” in *International Conference on Learning Representations*, 2015.
- [8] Nicholas Carlini and David Wagner, “Towards evaluating the robustness of neural networks,” in *2017 IEEE Symposium on Security and Privacy (SP)*. IEEE, 2017, pp. 39–57.
- [9] Naveed Akhtar and Ajmal Mian, “Threat of adversarial attacks on deep learning in computer vision: A survey,” *IEEE Access*, vol. 6, pp. 14410–14430, 2018.
- [10] Battista Biggio and Fabio Roli, “Wild patterns: Ten years after the rise of adversarial machine learning,” *Pattern Recognition*, vol. 84, pp. 317–331, 2018.
- [11] Awni Hannun, Carl Case, Jared Casper, Bryan Catanzaro, Greg Diamos, Erich Elsen, Ryan Prenger, Sanjeev Satheesh, Shubho Sengupta, Adam Coates, et al., “Deep speech: Scaling up end-to-end speech recognition,” *arXiv preprint arXiv:1412.5567*, 2014.
- [12] Yedid Hoshen, Ron J Weiss, and Kevin W Wilson, “Speech acoustic modeling from raw multichannel waveforms,” in *2015 IEEE International Conference on Acoustics, Speech and Signal Processing (ICASSP)*. IEEE, 2015, pp. 4624–4628.
- [13] Aaron van den Oord, Sander Dieleman, Heiga Zen, Karen Simonyan, Oriol Vinyals, Alex Graves, Nal Kalchbrenner, Andrew Senior, and Koray Kavukcuoglu, “Wavenet: A generative model for raw audio,” 2016.
- [14] Tara N Sainath, Ron J Weiss, Andrew Senior, Kevin W Wilson, and Oriol Vinyals, “Learning the speech front-end with raw waveform cldnns,” in *Sixteenth Annual Conference of the International Speech Communication Association*, 2015.
- [15] Mirco Ravanelli and Yoshua Bengio, “Speaker recognition from raw waveform with sincnet,” in *2018 IEEE Spoken Language Technology Workshop (SLT)*. IEEE, 2018, pp. 1021–1028.

- [16] Neil Zeghidour, Nicolas Usunier, Iasonas Kokkinos, Thomas Schaiz, Gabriel Synnaeve, and Emmanuel Dupoux, “Learning filterbanks from raw speech for phone recognition,” in *2018 IEEE International Conference on Acoustics, Speech and Signal Processing (ICASSP)*. IEEE, 2018, pp. 5509–5513.
- [17] Neil Zeghidour, Nicolas Usunier, Gabriel Synnaeve, Ronan Collobert, and Emmanuel Dupoux, “End-to-end speech recognition from the raw waveform,” *arXiv preprint arXiv:1806.07098*, 2018.
- [18] Nicholas Carlini and David Wagner, “Audio adversarial examples: Targeted attacks on speech-to-text,” in *2018 IEEE Security and Privacy Workshops (SPW)*. IEEE, 2018, pp. 1–7.
- [19] Seyed-Mohsen Moosavi-Dezfooli, Alhussein Fawzi, Omar Fawzi, and Pascal Frossard, “Universal adversarial perturbations,” in *The IEEE Conference on Computer Vision and Pattern Recognition (CVPR)*, July 2017.
- [20] Jonathan Peck, Joris Roels, Bart Goossens, and Yvan Saeys, “Lower bounds on the robustness to adversarial perturbations,” in *Advances in Neural Information Processing Systems*, 2017, pp. 804–813.
- [21] Ali Shafahi, W. Ronny Huang, Christoph Studer, Soheil Feizi, and Tom Goldstein, “Are adversarial examples inevitable?,” in *International Conference on Learning Representations*, 2019.
- [22] Alhussein Fawzi, Hamza Fawzi, and Omar Fawzi, “Adversarial vulnerability for any classifier,” in *Advances in Neural Information Processing Systems*, 2018, pp. 1178–1187.
- [23] Alexey Kurakin, Ian Goodfellow, and Samy Bengio, “Adversarial examples in the physical world,” in *International Conference on Learning Representations (workshop)*, 2017.
- [24] Anish Athalye, Logan Engstrom, Andrew Ilyas, and Kevin Kwok, “Synthesizing Robust Adversarial Examples,” in *International Conference on Machine Learning*, 2018.
- [25] Nicholas Carlini, Pratyush Mishra, Tavish Vaidya, Yuankai Zhang, Micah Sherr, Clay Shields, David Wagner, and Wenchao Zhou, “Hidden voice commands,” in *25th Security Symposium*, 2016, pp. 513–530.
- [26] Guoming Zhang, Chen Yan, Xiaoyu Ji, Tianchen Zhang, Taimin Zhang, and Wenyuan Xu, “Dolphinattack: Inaudible voice commands,” in *Proceedings of the 2017 ACM SIGSAC Conference on Computer and Communications Security*. ACM, 2017, pp. 103–117.
- [27] Yuan Gong and Christian Poellabauer, “Crafting adversarial examples for speech paralinguistics applications,” *arXiv preprint arXiv:1711.03280*, 2017.
- [28] Corey Kereliuk, Bob L Sturm, and Jan Larsen, “Deep learning and music adversaries,” *IEEE Transactions on Multimedia*, vol. 17, no. 11, pp. 2059–2071, 2015.
- [29] Tianyu Du, Shouling Ji, Jinfeng Li, Qinchen Gu, Ting Wang, and Raheem Beyah, “Sirenattack: Generating adversarial audio for end-to-end acoustic systems,” *arXiv preprint arXiv:1901.07846*, 2019.
- [30] Moustafa Alzantot, Bharathan Balaji, and Mani Srivastava, “Did you hear that? adversarial examples against automatic speech recognition,” *arXiv preprint arXiv:1801.00554*, 2018.
- [31] Tara Sainath and Carolina Parada, “Convolutional neural networks for small-footprint keyword spotting,” 2015.
- [32] Hiromu Yakura and Jun Sakuma, “Robust audio adversarial example for a physical attack,” *arXiv preprint arXiv:1810.11793*, 2018.
- [33] Yao Qin, Nicholas Carlini, Ian Goodfellow, Garrison Cottrell, and Colin Raffel, “Imperceptible, robust, and targeted adversarial examples for automatic speech recognition,” *arXiv preprint arXiv:1903.10346*, 2019.
- [34] Seyed-Mohsen Moosavi-Dezfooli, Alhussein Fawzi, Omar Fawzi, Pascal Frossard, and Stefano Soatto, “Robustness of classifiers to universal perturbations: A geometric perspective,” in *International Conference on Learning Representations*, 2018.
- [35] Jan Hendrik Metzen, Mummadi Chaithanya Kumar, Thomas Brox, and Volker Fischer, “Universal adversarial perturbations against semantic image segmentation,” in *2017 IEEE International Conference on Computer Vision (ICCV)*. IEEE, 2017, pp. 2774–2783.
- [36] Melika Behjati, Seyed-Mohsen Moosavi-Dezfooli, Mahdih Soleymani Baghshah, and Pascal Frossard, “Universal adversarial attacks on text classifiers,” in *ICASSP 2019-2019 IEEE International Conference on Acoustics, Speech and Signal Processing (ICASSP)*. IEEE, 2019, pp. 7345–7349.

- [37] Jamie Hayes and George Danezis, “Learning universal adversarial perturbations with generative models,” in *2018 IEEE Security and Privacy Workshops (SPW)*. IEEE, 2018, pp. 43–49.
- [38] Jérôme Rony, Luiz G Hafemann, Luiz S Oliveira, Ismail Ben Ayed, Robert Sabourin, and Eric Granger, “Decoupling direction and norm for efficient gradient-based l2 adversarial attacks and defenses,” *arXiv preprint arXiv:1811.09600*, 2018.
- [39] Seyed-Mohsen Moosavi-Dezfooli, Alhussein Fawzi, and Pascal Frossard, “Deepfool: a simple and accurate method to fool deep neural networks,” in *Proceedings of the IEEE conference on computer vision and pattern recognition*, 2016, pp. 2574–2582.
- [40] Diederik P Kingma and Jimmy Ba, “Adam: A method for stochastic optimization,” *arXiv preprint arXiv:1412.6980*, 2014.
- [41] John Duchi, Elad Hazan, and Yoram Singer, “Adaptive subgradient methods for online learning and stochastic optimization,” *Journal of Machine Learning Research*, vol. 12, no. Jul, pp. 2121–2159, 2011.
- [42] Ilya Sutskever, James Martens, George Dahl, and Geoffrey Hinton, “On the importance of initialization and momentum in deep learning,” in *International conference on machine learning*, 2013, pp. 1139–1147.
- [43] Ian Goodfellow, Yoshua Bengio, and Aaron Courville, *Deep Learning*, MIT Press, 2016, <http://www.deeplearningbook.org>.
- [44] J. Salamon, C. Jacoby, and J.P. Bello, “A dataset and taxonomy for urban sound research,” in *22nd ACM International Conference on Multimedia*, New York, NY, USA, 2014, pp. 1041–1044.
- [45] Sajjad Abdoli, Patrick Cardinal, and Alessandro Lameiras Koerich, “End-to-end environmental sound classification using a 1d convolutional neural network,” *arXiv preprint arXiv:1904.08990*, 2019.
- [46] Yuji Tokozume, Yoshitaka Ushiku, and Tatsuya Harada, “Learning from between-class examples for deep sound recognition,” *arXiv preprint arXiv:1711.10282*, 2017.
- [47] Karen Simonyan and Andrew Zisserman, “Very deep convolutional networks for large-scale image recognition,” *arXiv preprint arXiv:1409.1556*, 2014.
- [48] Seyed-Mohsen Moosavi-Dezfooli, Alhussein Fawzi, Omar Fawzi, and Pascal Frossard, “Universal adversarial perturbations,” in *Proceedings of the IEEE conference on computer vision and pattern recognition*, 2017, pp. 1765–1773.
- [49] Yanpei Liu, Xinyun Chen, Chang Liu, and Dawn Song, “Delving into transferable adversarial examples and black-box attacks,” in *International Conference on Learning Representations*, 2017.
- [50] Aleksander Madry, Aleksandar Makelov, Ludwig Schmidt, Dimitris Tsipras, and Adrian Vladu, “Towards deep learning models resistant to adversarial attacks,” in *International Conference on Learning Representations*, 2018.
- [51] Matthew D. Zeiler, “Adadelata: An adaptive learning rate method,” 2012.
- [52] N. Srivastava, G.E. Hinton, A. Krizhevsky, I. Sutskever, and R. Salakhutdinov, “Dropout: a simple way to prevent neural networks from overfitting,” *Journal of Machine Learning Research*, vol. 15, no. 1, pp. 1929–1958, 2014.
- [53] Sergey Ioffe and Christian Szegedy, “Batch normalization: Accelerating deep network training by reducing internal covariate shift,” *arXiv preprint arXiv:1502.03167*, 2015.
- [54] Jimmy Lei Ba, Jamie Ryan Kiros, and Geoffrey E Hinton, “Layer normalization,” *arXiv preprint arXiv:1607.06450*, 2016.
- [55] Andrew L Maas, Awni Y Hannun, and Andrew Y Ng, “Rectifier nonlinearities improve neural network acoustic models,” in *Proc. icml*, 2013, vol. 30, p. 3.